Coronal Mass Ejections and Type II Radio Bursts

Henry Aurass

Astrophysikalisches Institut Potsdam, Observatorium für solare Radioastronomie, Telegrafenberg A31, D - 14473 Potsdam, Germany

Abstract. Coronal mass ejections (CMEs) and shock wave induced radio bursts (type II) are reviewed. CMEs are - beneath flare blast waves - invoked to be the drivers of type II burst emitting super-Alfvénic disturbances. The paper focuses on the available experimental evidence for this assumption. For instance, the apparent contradiction is discussed between measured speeds of potential shock drivers and their observed type II burst association. Further, several examples are presented for recognizing CMEs by the appearance of other characteristic nonthermal radio signatures. Open problems are assembled which should be newly attact by high time and frequency resolution decimeter and meter wave radio spectral and imaging observations from ground combined with visible light and X-ray imaging data from YOHKOH and SOHO space experiments. The paper shows that radio observations in general, and especially the radiation of shock accelerated electrons, constitute a unique access to the structure and the dynamics of the coronal magnetoplasma. This is important for understanding the timing and the sites of energy release processes in the solar corona and for studying the physics of collisionless shock waves in space plasmas.

Résumé. Nous présentons une revue des caractéristiques observationnelles des éjections de matière coronale (EMC's) et des ondes de choc dont les signatures sont des sursauts radio de type II. Il est généralement admis que EMC's et ondes de choc explosives, associées aux éruptions, sont à l'origine des perturbations superalfveniques qui engendrent les type II. Touutefois il existe un désaccord apparent entre les vitesses mesurées pour EMC's et ondes explosives et celles des sursauts de type II. Magré cela, nous montrons sur des exemples que certaines émissions radio non-thermiques constituent des signatures des EMC's. De plus nous identifions un ensemble de problèmes pour lesquels la combinaison d'observations radio decimétrique-métrique, obtenues au sol avec de hautes résolutions temporelle, spectrale et spatiale, avec l'imagerie en lumière blanche et en rayons X, fournie par des instruments embarqués sur les satellites SOHO et YOHKOH, devraient permettre de mieux cerner. Plus généralement nous tentons de montrer que les observations radio, et plus particulièrement celles générées par les électrons accélérés par les chocs, fournissent un moyen unique pour étudier la structure et la dynamique du magnéto-plasma coronal. Ceci est important pour: (i) caractériser l'évolution temporelle et localiser les sites de la libération d'énergie dans la Couronne; (ii) étudier la physique des ondes de choc non collisionnelles dans les plasmas naturels.

1 Introduction

Solar flares and solar coronal mass ejections - CMEs - (or coronal magnetic ejections, Hundhausen 1995) are energetically the most important transient phenomena of the solar atmosphere. Both can initiate - either as an expanding blast wave or as an escaping massive piston - a moving MHD-like disturbance which grows in the solar corona (and/or later in the solar wind) to a collisionless shock wave if its speed is larger than the local Alfvén velocity in the background atmosphere. In the meter wave range (300 - 30 MHz) radio spectral observations reveal slowly drifting features (type II bursts). This is usually taken as evidence of super-Alfvénic disturbances. Type II bursts are then the radio signature of energetic electrons (up to tens of keV) accelerated at flare or CME related shock waves. It should be emphasized that radio emission of shock-accelerated particles is the only ground based observational access to coronal shock waves. From spacecraft, in-situ observations of shock front passages and remote sensing of low frequency (hectometer) shock-associated radio emission are possible in the solar wind (see e.g. Bougeret 1985 for a review).

There is a gap between ground and space based radio observations of type II bursts caused by the ionosphere, the probably low intensity of shock related radio emission below 20 MHz, and the high radio background in this range. Only the recently flown CORONAS I and WIND/WAVES experiments provided a sufficient overlap with the frequency range accessible from ground. However, an example of a continuous tracing of a radio visible shock from meter waves down to hectometer waves has not yet been reported in the literature. It is well possible that coronal and interplanetary radio shock signatures must not appear together, and could have different drivers within one solar event (especially in the case of a flare associated CME).

Shocks and CMEs are quoted by the solar energetic particle community as accelerators of MeV electrons and protons, but the details of how to get such high energies under coronal conditions are not yet properly understood (Mann, pers. comm.). Notice that Klein et al. (1988) and Klein et al. (1995) have shown that extended coronal shocks play a minor part in the acceleration of relativistic electrons observed in the low corona.

At present two solar oriented space missions offer a new quality of imaging observations of the solar corona:

- The soft X-ray telescope (SXT) onboard the YOHKOH mission (first data September 1991) presents high cadence images (Tsuneta et al. 1991) of hot and dense coronal magnetoplasma structures;
- The SOHO mission (first data April 1996) includes the first orbiting coronograph (LASCO, Brückner et al. 1995) working down to a height of 0.1 $R_\odot$ above the photosphere.

Both these new space experiments provide detailed information about structure and motions of the coronal magnetoplasma. Both cover the same height

range in which the nonthermal decimeter and meter wave radio burst sources are located. This provides a new opportunity to investigate the potential of existing ground based solar observations which, in the contrary, are sensitive to nonthermal electrons energized during transient solar phenomena.

There is a large amount of previous work about solar radio type II bursts on the one hand and about the relationship of radio phenomena with the appearance of CMEs in white light observations on the other hand (for a summary see e.g. Hildner et al. 1986, and Section 2 of the present paper). Definitive results about radio phenomena associated with CMEs are mainly obtained by radio imaging facilities at low frequencies - the Culgoora Heliograph (160, 80, 43 MHz, for an instrumental description see Labrum 1985), the Clark Lake Radioheliograph (120 - 25 MHz, see Kundu et al. 1983), and the Nançay Radio Heliograph - NRH - (The Radioheliograph Group 1993). At present, the NRH is the only working meter wave imaging facility dedicated to the sun. A complete review of all these radio physical results is beyond the scope of this paper. Published work shows that the observation of shock- and CME related radio phenomena requires simultaneous high time and spectral resolution in the whole meter and decimeter range combined with imaging data of comparable time resolution on at least two frequencies within the range of spectral observations. In Europe, the NRH working at five frequencies with 0.1 s time resolution combined e.g. with the Potsdam-Tremsdorf 40 - 800 MHz spectrometer system (Mann et al. 1992) are best fitting the given instrumental demands. During the flight of YOHKOH and SOHO this gives a promising perspective for association studies.

In Section 2 some aspects of CMEs and of the radio signature of coronal shock waves are briefly reviewed. In Section 3 some answers are assembled to the question "How to see a CME in radio?".

2 Summary About CMEs and Coronal Shock Waves

In recent years several reviews concerning CMEs have been published. We refer to Harrison (1991), Kahler (1992), Steinolfson (1992), Chertok (1993), Low (1993), Webb (1994), Dryer (1994), Hundhausen (1994), Webb et al. (1994), and Hundhausen (1995). For reviews about the radio signature of coronal shock waves see e.g. Bougeret (1985), Aurass (1992), and Mann (1995a). This paper focuses on common aspects of CMEs and coronal shock waves and on nonthermal radio signatures of both phenomena.

2.1 Coronal Mass Ejections

Morphology. A coronal mass ejection appears on white light coronograph images as brightening, blowing up and ejection of a more or less extended region of the solar corona. Despite the fact that CMEs have been observed for 20 years they are not yet fully understood. CMEs reveal a large scale

evolutionary process of reconfiguration of the coronal magnetic field (Sime 1989).

Burkepile and St. Cyr (1993) have shown impressive CME images and have reported statistical information about the different CME forms. One third of all CMEs consists of the typical structural elements of the loop or bubble type. The outermost feature is a bright leading arch, followed by a dark cavity and a bright core of dense matter. The bright core is usually identified with parts of an uplifting filament, the dark cavity might be the disconnected coilshaped flux system which was supporting the filament before. There are also such CMEs without a bright core. About a quarter of all CMEs consists of a diffuse brightness enhancement (type "material" or "cloud"). A further 25 % of CMEs have very different but well defined forms. According to Kahler (1991) "...typical CMEs tend to occur in streamer structures and destroy or significantly modify these structures ...". Only 1.9 % of all CMEs are themselves formed like streamers. Coronal helmet streamer latitudes and CME latitudes have coincident scatterplots over the solar activity cycle (Hundhausen 1993). But the presence of a streamer structure is not necessary for CME formation. For near-minimum conditions Kahler (1991) found CMEs associated with an active region without an overlying streamer structure, and streamers over active regions without a CME.

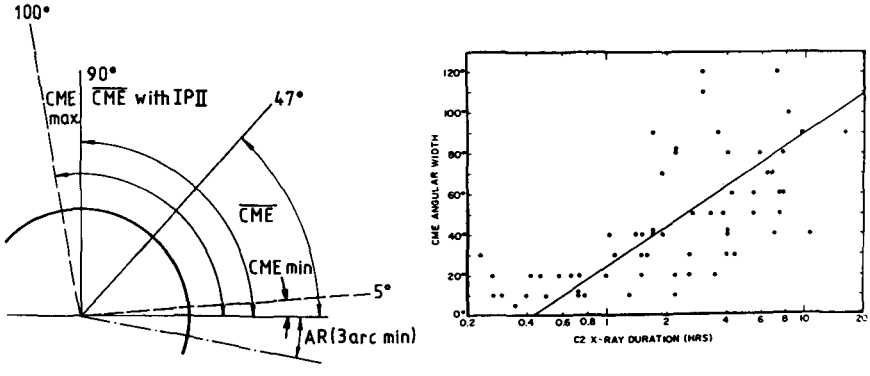

Fig. 1. a - left: The spatial scale of CMEs acording to Hundhausen (1993) and Cane et al. (1987). AR means active region. b - right: The linear relation between the log. duration of an soft X-ray burst and the span of the associated CME (from Kahler et al. 1989).

Figure 1a summarizes the information about the angular span of CMEs as given by Hundhausen (1993) and using Cane et al. (1987). Three facts are of special importance for analyzing associations between CMEs and flare (active region) related phenomena:

- The angular extent of an average CME is nearly five times larger than a medium size active region.
- The smallest CMEs have about the same span as an active region.
- Those CMEs which are associated with a low frequency interplanetary type II burst are on average twice as large as a typical CME.

Association with Soft X - Ray Phenomena. There is a statistically confirmed relationship between the angular extent of a CME and the duration of the simultaneously observed soft X-ray burst (Kahler et al. 1989 and our Figure 1b). This means on average the spatial scale of a CME determines the time scale of an associated energy dissipation process (e.g. heating) in the corona. Hundhausen (1995) points the attention on some exceptional examples.

What is known about the time sequence and the spatial relation of CMEs and associated X-ray sources ?

Harrison et al. (1990) report on minor X-ray events leading in time the CME onset and the onset of the associated main X-ray burst. The time interval between minor and main X-ray event is of the order of tens of minutes. This is the same time scale as given for early nonthermal energy release signatures in microwaves (Kai et al. 1983) and decimeter waves (Averianikhina et al. 1990).

One of the discoveries of the YOHKOH mission results from SXT's ability to see CME related features on the disk. Hiei et al. (1993) report on coronal mass loss observations during a high latitude arcade event. Hudson (1995) describes a structured soft X-ray cloud adjacent to a flare on the disk which starts moving and disappeares completely within 1 hour. McAllister et al. (1994, 1996) present evidence for a polar crown CME which passed by the Ulysses spacecraft and caused a strong geomagnetic storm. No flare and evident soft X-ray flux change, nor a big prominence disappearance was noticed. Within 10 hours after the probable solar ignition of the event, a faint but very elongated (150 degs in longitude and 30 degs in latitude !) X-ray arcade was formed between coronal hole boundaries and above a highly warped magnetic neutral line. The only feature resembling to flare activity were He 10830 ribbons at the arcade footpoints.

In YOHKOH images, Švestka et al. (1995) have recognized hints on to the process of arcade formation in its vertical extent - the long duration growth of giant X-ray arches. These arches were already discovered in SMM X-ray images. Švestka et al. (1995) argue from the analysis of 7 events that the expanding giant arches are a consequence of (or at least associated with) CMEs. In extension of the H_α post flare loop evolution, the giant arches grow with constant speeds between 1.1 and 12.1 $km\,s^{-1}$. They represent relatively strong density enhancements which slowly decay with time. For one example, there is a fivefold density decrease reported over a time interval of 11.5 hours

which corresponds with a giant arch volume expansion rate of 0.7 % per minute. We come back to this result in Section 3.

The observations point to the relevance of Kopp and Pneuman's (1976) model of field line reclosure due to magnetic reconnection after prominence eruptions for understanding CMEs. For a detailed comparison of soft X-ray and white light coronal features it is important that the LASCO system onboard SOHO will cover the same height range in which the soft X-ray giant arches have been observed. This is in contrast with the SMM coronograph.

Other Associations. The discussion about the spatial scales of CMEs is a suitable point to ask generally for associations of CMEs with other classes of solar activity. Webb and Howard (1994) reanalysed the data of all orbiting coronographs. They found that no one class of solar activity is better correlated with the CME rate over the solar activity cycle than any other.

An important point is the relationship of CMEs to flares and to active regions. As already noted (Figure 1a) the angular span of an average CME is at least 5 times larger than active region magnetic field structures in the corona. Only the smallest CMEs start on spatial scales which are comparable to flare structures. The association of a CME with an erupting active region filament is simple only in cases of spatially narrow CMEs. If a broad CME is associated with a flaring active region it can be situated anywhere under the arch spanned by the CME (Harrison et al. 1990). Kahler (1991) found under minimum solar activity conditions equator-crossing CMEs rooted in two active regions.

As already mentioned a CME can be accompanied by the disappearance of quiescent filaments (e.g. Mouradian et al. 1996) and by flares. Not all features existing in the disturbed corona behind the leading parts of the white light CME need to be visible in white light images, some of them - e.g. the erupting filament, the moving type IV burst, the magnetic field structures in the lower corona - are discussed in the flare context, too. This may be a source of terminology confusion.

2.2 Coronal Shock Waves

All experimental facts about shock waves in the solar corona result from remote sensing in the meter wave range. This is possible due to the fact that coronal shocks accelerate electrons to energies of several tens of keV leading to an enhanced level of high frequency plasma wave turbulence. The high frequency (Langmuir or upper hybrid) waves can be scattered off ions or off low frequency plasma waves (e.g. ion sound). Further, they can coalesce with other high frequency waves. Thus one gets radio emission of type II near the local plasma frequency (f_p, F) and/or its second harmonic (2 f_p, H). For type II burst terminology see Nelson and Melrose (1985) and Aurass (1992).

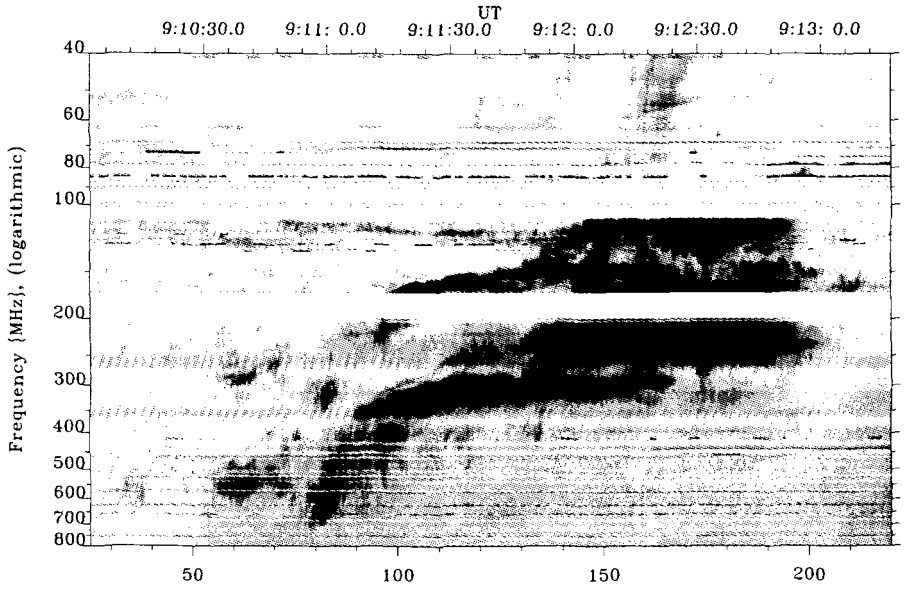

Fig. 2. The type II burst of 09 July 1996.

Spectral Data. Figure 2 shows a digitally processed type II burst spectrogram (background subtracted). Stripes parallel to the time axis are terrestrial transmitters. Note the high starting frequency (350 MHz for the F lane) and the complex and multiple lane pattern. Figure 3 presents the fundamental lane of a type II burst with extremely strong herringbone structure. There is also a backbone interval without herringbones (12:11:22 - 35). This reveals that the backbone is an independent component and not a superposition of herringbones.

Aurass et al. (1994a) find several examples for type II bursts with three harmonically related lanes. Together with the usual F and H lanes there appears a lane at thrice the plasma frequency ($3\ f_p$). After early reports (Aurass 1992 and references therein) it is now a well-proven experimental fact that type II emission at the third harmonic of the plasma frequency is not as rare and doubtful as believed earlier. An extended investigation (Zlotnik et al., this conference) reveals a brightness temperature ratio from 4 to 1000 between the H and the third harmonic source.

According to common knowledge (e.g. Švestka 1976) the ignition of the type II emitting disturbance can drive a Moreton wave in the photosphere. The launch time of flare associated shocks was newly analysed in a statistical study about type II bursts starting at high frequencies (Vršnak et al. 1995). The result favours a launch time prior to the first peak of the associated microwave burst. Karlický and Odstrčil (1994) describe type II burst related

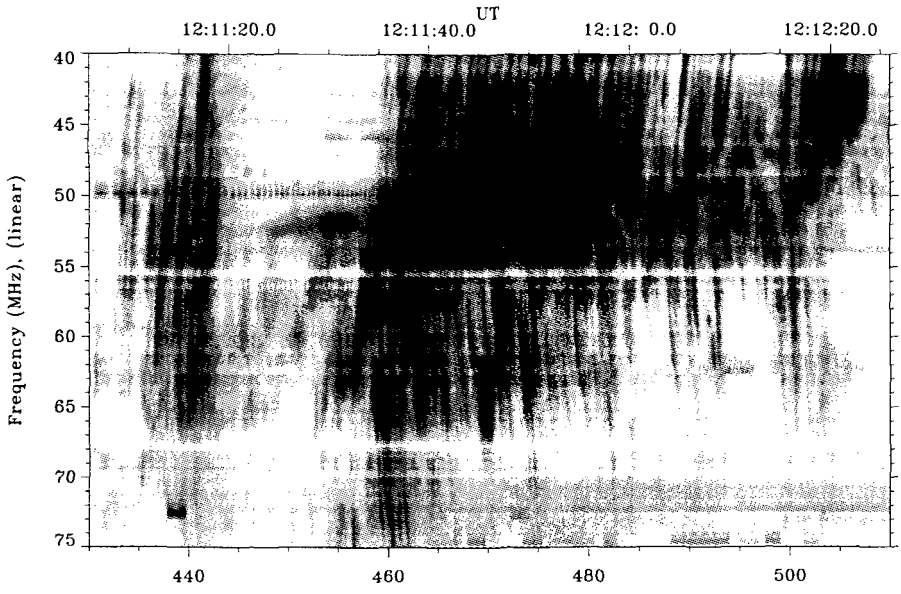

Fig. 3. The type II burst of 30 June 1995 with strong herringbone fine structure in the fundamental lane.

features seen above 1 GHz. Aurass et al. (1994b) study a typical pattern of decimetric emission with a triangular envelope (a trianglar spectral pattern, TSP) in the radio spectra which was found to systematically preceede some type II bursts and becomes possibly several times visible in the spectrum with delays of 3 to 4 minutes between. In Figure 4 we show two examples of this effect. Here, the TSP together with some type III bursts is the earliest feature of the event to precede the impulsive microwave and γ-ray burst. In this example the second TSP immediately precedes the type II burst lanes. The data support the idea that for some flares the type II burst emitting disturbance is initiated by energy release processes in large coronal heights. Klassen (1996) presents a TSP which interferes with a superposed pair of a type III and a reverse drift burst appearing in absorption on the TSP background. This leads to the conclusion that this TSP was exited near a cusp-shaped magnetic field structure. Tsuneta (1996) has recently emphasized the importance of cusp-shaped structures for the flare process.

In studying type II bursts several questions arise, e.g.

- What is the thickness of the shock transition region under coronal conditions ?
- What is the site of radio emission in the shock reference frame ?
- Where are the sites of particle acceleration at the shock front ?

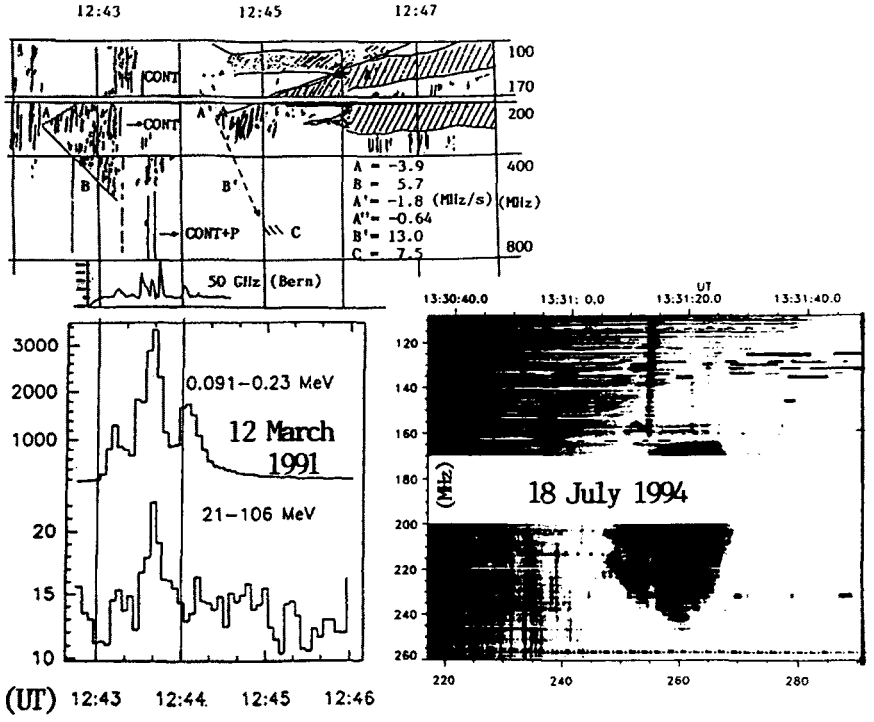

Fig. 4. Two examples of triangular spectral patterns. Left: Event 12 March 1991, top: sketch of the dynamic spectrum observed at Potsdam-Tremsdorf. Middle: the microwave burst (from Aurass et al. 1994b) and (bottom) the high energy emission (Vilmer 1993) begin 30 s past the first TSP. The second TSP precedes the type II lanes. Right: the TSP preceding the 18 July 1994 type II burst (from Klassen 1996).

The transition region of a collisionless shock has a thickness of several ion inertial lengths (cf. Mann et al. 1995 and references therein). The ion inertial length is a plasma parameter (Krall and Trivelpice 1973) ranging from about 7 m at a plasma frequency level of 300 MHz (low corona) to about 100 km (plasma frequency level of 20 kHz, solar wind plasma at 1 AU). This means the shock transition region of coronal disturbances is a thin surface of some tens of meters width which cannot be resolved by radio imaging instruments. We assume that fast mode shocks are the most probable source of type II bursts among those possible in the corona (Mann et al. 1995). Then its transition region is characterized by a positive jump of the magnetic field strength, the temperature and the density. The mean instantaneous

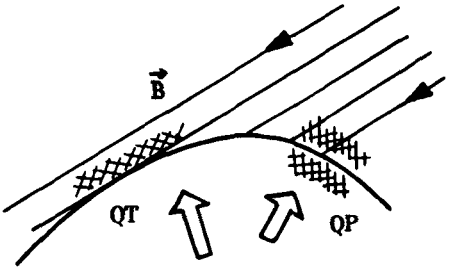

Fig. 5. Scheme of a shock wave with quasi-parallel (QP) and quasi-transversal (QT) transition intervals. Regions of particle acceleration are cross-hatched (according to Mann and Claßen 1995).

bandwidth of type II bursts (about 30 %, Mann et al. 1996) leads to an average density jump of 74 % of the background. The shock transition region represents a strong density jump which becomes visible as plasma emission of shock accelerated electrons. The frequency of plasma emission depends on the density - therefore a highly resolved spectrum in time and frequency offers a look into otherwise unobservable spatial scales. Of course it is impossible to read this information without theoretical guidelines.

From in-situ observations of shock waves in the interplanetary space (Mann et al. 1995 for references) it is known that high frequency plasma waves are mainly concentrated in the upstream region. Low frequency plasma waves dominate in the downstream region. Since both components are necessary for the formation of escaping radio emission Mann et al. (1995) conclude that the radio source region must be situated at the overlap of both components - at the shock transition.

In Figure 5 we have sketched a shock front and the upstream field lines of the background magnetic field. "QT " is a quasi-transversal shock, "QP " characterizes a quasi-parallel shock transition. The shock drift acceleration process (see Holman and Pesses 1983, Benz and Thejappa 1988) acts immediately in front of the QT transition region (cross-hatched in Figure 5). The energy of the accelerated electrons depends sensitively on the angle between the shock normal and the magnetic field. For getting the necessary energies to explain the backbone emission, but much more for getting particle speeds consistent with herringbone data (e.g. Mann and Klose 1995) a very sharp angular criterion has to be fullfilled. For the observer, it looks strange to assume that during several minutes of type II burst duration the mentioned angle should persist e.g. between 88 and 90 degrees, given the structural complexity of the coronal magnetoplasma. This problem has been resolved recently by

Mann et al. (1994) and Mann and Claßen (1995) presuming that the same basic physical processes act at collisionless shocks in different space plasmas. They assume that QP shock waves are - in the same manner as at the earth's bow shock - represented by an ensemble of short large amplitude magnetic field structures (SLAMS, cross-hatched in Figure 5) appearing in the upstream and the downstream region. SLAMS have an amplitude-dependent relative speed in the shock reference frame (Mann, 1995b). Therefore they can act as moving magnetic mirrors. Mann and Claßen (1995) show that also at QP shock waves electron acceleration is possible up to high energies.

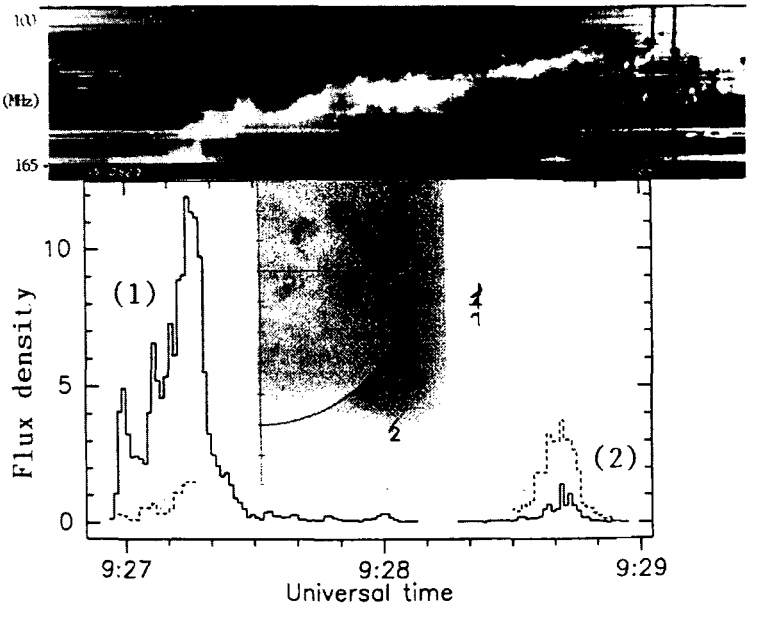

Fig. 6. An example for the type II burst large scale source structure. For explanations see text.

Imaging Data - the Source Structure of Type II Bursts. Early reports from Culgoora observations deal with large ($\gtrsim 0.5\ R_\odot$) sources consisting of different archlike distributed subsources (Nelson and Melrose 1985 for detailed reference). According to recent experience it is impossible to judge about the source structure without an exact spectral identification. For illustration we present in Figure 6 a simple example (from Aurass et al. 1994a). The type II burst spectrum shows a single lane (probably the H lane, Figure 6 top between 100 and 165 MHz). The lane consists of two split bands with

variable split bandwidth. The high frequency split band enters the given spectral range nearly 1.5 minutes later than the low frequency split band. This offers the opportunity to discriminate clearly the radio images of both split bands at the 164 MHz NRH observing frequency. The middle part of Figure 6 shows the corresponding source distribution. Only the source centers have been drawn for simplicity.

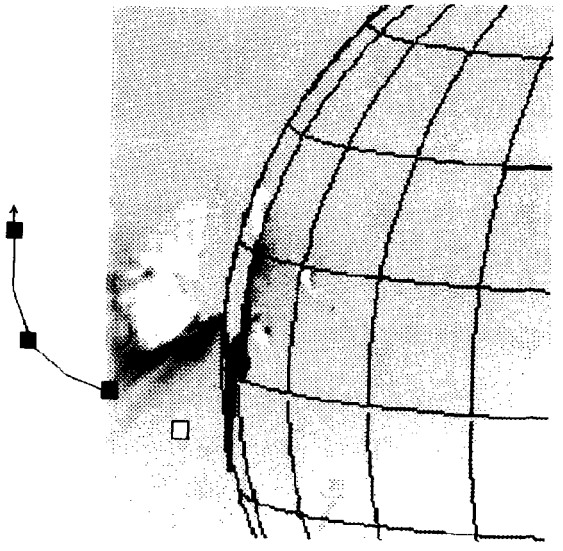

Fig. 7. The gross source structure of the type II burst of 27 September 1993 near the west limb which had a strong third harmonic lane (the spectrum is shown e.g. in Aurass et al. 1994a). The sources are superposed to a YOHKOH SXT difference image (see text). Open square: strong F and faint H source in the beginning of the type II burst. The nearest black square (on the X-ray image boundary): strong H and faint F as well as 3F source in the beginning of the type II burst. Further black squares: trace of the main H and the 3F source later in the burst.

The radio sources appear pairwise for each split band with about 0.5 $R_\odot$ distance between the source sites. They are superposed on to a YOHKOH SXT image and are situated on both sides of a large soft X-ray loop structure. During the passage of both split bands over the 164 MHz plasma level the NRH indicates a simultaneous brightening at both source sites with different weights. In the bottom of Figure 6 the flux curves (in arbitrary units for both sources 1, 2) are given. Recall that the band splitting reflects local properties of the wave front. It allows us to infer the density jump in the shock transition region which is a distance of some tens of meters under coronal cir-

cumstances. On the other hand both split bands in the spectrum are formed from contributions of widely separated source sites. We argue that there is a common electron population propagating along the shock front and / or along the field lines of the loop seen in soft X-rays. The changing intensity weight of both sources for the different split bands can be a directivity effect for electron streams or radio emission. This finding demands for a systematic investigation.

The discussed simple example confirms that for understanding more complex type II spectra combined high spectral and time resolution data are inevitably necessary for associating the (seemingly) complex spatial pattern of subsources with the correct spectral structure. Further, we stress that in the case of a somewhat lower sensitivity of the imaging instrument one would see for each split band one source, only (No. 1 for the low frequency split band, No. 2 for the high frequency split band, comp. Figure 6) with a large distance between. It is well possible that this finding explains some of the earlier reported discrepancies about the relative position of different spectral features of type II bursts (Dulk 1982, Nelson and Melrose 1985).

Aurass et al. (1994a) have first shown imaging data of a type II burst at three harmonically related frequencies (Figure 7). For the F and H lanes again a double source has been found for comparable spectral substructures. For this event, a clear image discrimination between the split band lanes is not possible. If measured at the same time on different frequencies the stronger F source is at the same site as the fainter H source and vice versa. The third harmonic source is single and appears at the same site as the main H source. These facts are consistent with the fundamental/harmonic interpretation and argue against significant effects of wave propagation on the radio emission at the analysed frequencies. Given the spectral extent of the event in relation with the NRH spectral coverage, in Figure 7 the sources can be shown initially for the F and the H lane, in later time intervals for the H and third harmonic source, only. Both move together on an appearantly archlike azimuthal path.

The radio sources are superposed on to a YOHKOH SXT difference image taken with the AlMg filter, 5 s exposure time, from the time before and after the flare (12:37 - 12:00 UT, without correction for solar rotation). The radio sources are all situated in a region which is hotter and denser after the flare.

Relation between Type II Source Positions and White Light CMEs. The large scale shock structure along the shock transition is of principal interest in searching for magnetoplasma structures in the solar corona. It is also important for recognizing the driving agent (blast wave or piston) of the shock and might be connected with the microphysical aspect of the processes in the shock front (acceleration processes, directivity of electron streams). Simultaneous observations of CMEs and the position of type II bursts are

the only way to determine the spatial relationship between both effects. Further this provides two independent approaches for density estimation in the disturbed coronal plasma.

Despite all efforts there were no simultaneous observations during the SKYLAB experiment (Hildner et al. 1986). Gopalswamy and Kundu (1992a) counted "...a dozen CME events with simultaneous radio and optical coverage". Therefore it is not surprising that there is no clear and unique picture about the CME / type II relation until now. Gary et al. (1985) present a type II burst with sources below the top of loop structures within a CME. Gergely et al. (1984) describe a CME with a type II burst source moving tangentially along CME loop structures toward the solar disk. Kundu and Gopalswamy (1992) report on a type II source in front of a CME, and Gopalswamy and Kundu (1989) discuss a clearly flare related type II burst behind a CME. A flare induced disturbance launching during a possibly associated CME in progress seems to be best fitting the coronal type II burst data. In contrast there is evidence for low frequency type II bursts in the interplanetary space to be driven by the most massive, energetic and fastest CMEs acting like pistons (Cane et al. 1987).

2.3 The Speed Problem

The apparent speeds of CMEs (Hundhausen et al. 1994) range from 10 to 2100 $\mathrm{km\,s^{-1}}$ with a mean value of 349 $\mathrm{km\,s^{-1}}$ (all features) and 445 $\mathrm{km\,s^{-1}}$ (only the "outer loop feature"). The average apparent speed of type II bursts is about 700 $\mathrm{km\,s^{-1}}$ (Robinson 1985). For the transformation of the drift rate (the measured quantity in the spectral records, $D_\mathrm{f} = df/dt$) in the exciter speed v_exc one implies a density model $\mathrm{N_e(s)}$ and an assumption about the angle between the velocity vector and the density gradient according to

$$D_\mathrm{f} = \frac{df}{dt} = \frac{1}{2\pi} \cdot \frac{d\omega_\mathrm{pe}}{dt} = \frac{f}{2} \cdot \frac{v_\mathrm{exc}}{L} \cdot \cos\left(\frac{dN_\mathrm{e}}{ds}, v_\mathrm{exc}\right) \qquad (1)$$

Here $\omega_\mathrm{pe} = \sqrt{4\pi e^2 N_\mathrm{e}/m_\mathrm{e}}$ is 2π times the plasma frequency, L is the coronal density height scale, m_e is the electron mass, N_e is the electron number density, and e is the elementary charge.

Although it seems to be trivial, we note that low drift rates need not mean low exciter speeds. Characterized by the typical F/H pattern in the spectrum it is easy to find type II burst lanes with zero drift rate. Urbarz (pers. comm.) found 27 out of more than 400 type II bursts with drift rates ≤ 0 in the Weissenau spectral data between 1974 and 1987. Already Weiss (1963) and Gergely et al. (1984) have drawn the attention on very low drift rate type II bursts with large tangential source motions. Zero drift spectra reveal a disturbance growing to a shock wave only on that part of its path

through the coronal plasma which is perpendicular to the coronal density gradient. Simplifying one could use the term azimuthal propagation in contrast with the mostly implied radial propagation.

A travelling collisionless MHD disturbance grows to a shock if the Alfvén speed of the background medium is smaller than the velocity of the disturbance. The local Alfvén speed v_A depends on the ratio of the magnetic field strength to the square root of the density - the disturbance grows to a shock in regions of $v > v_A = 2.1 \cdot 10^6 \cdot B/\sqrt{N_e}$ (B in 10^5 nT, N_e in cm^{-3}). Characteristic values for the Alfvén speed are about 500 $km\,s^{-1}$ in the lower corona (at the 300 MHz plasma level assuming $B = 10^6$ nT) and 60 $km\,s^{-1}$ in the solar wind at 1 AU (at the 20 kHz plasma level assuming $B = 6$ nT). In the solar wind the disturbance must additionally overcome the background streaming velocity of 470 $km\,s^{-1}$ (mean value). Assuming the CME drives the disturbance, only fast CMEs should be associated with a type II burst. But this is not true: Gopalswamy and Kundu (1992) present a list of 6 cases of slow CMEs (speeds below 400 $km\,s^{-1}$) accompanied by a type II burst in the corona. On the other hand, Sheeley at al. (1984) show a histogram of 34 CMEs being - despite a broad velocity scatter between 200 and 1600 $km\,s^{-1}$ - without metric type II bursts. These facts underline and confirm that the appearance of a type II burst is not only determined by the disturbance velocity. There must be strong differences in the Alfvén speed of the plasma surrounding the source of the disturbance. This is a way to understand that in some flares the metric type II burst appears suddenly at relatively low frequencies - this would then only reflect the inhomogenity around the exciter and not a large height in the corona.

As proposed already by Uchida (1974) channeling of the disturbance appears into low v_A regions if the background Alfvén speed is inhomogeneous. The results of a statistical study by Person et al. (1989) show that the appearance of a coronal type II burst does not depend on the energy of the exciting flare and therefore point in the same direction. Aurass and Rendtel (1989) compare the type II burst productivity of two very flare active regions. They find that a coronal hole - with low Alfvén speed inside - in the immediate surroundings of one region could be the cause for the significantly enhanced number of type II bursts induced by the flares in this region. There is still another observational argument. Recall Figure 1a - those CMEs which are associated with a kilometric type II burst in the solar wind are on average twice as large as the average CME. Presuming an inhomogeneous solar wind a large angular span of the disturbance enhances the probability to meet low v_A regions. This is the effect which Kahler et al. (1984) could not find in the lower corona.

Summarizing: type II bursts can be the radio illumination of low v_A regions of the inhomogeneous corona independently from driving the shock by a piston (e.g. a CME) or getting the shock from a semi-spherically escaping flare blast wave. The relatively sparse data about the position of the

CME's leading edge to the type II burst sources seem to be in favour of a flare excited driver of the coronal shock wave. The same can be argued from the average CME - flare - type II onset timing. This conclusion is already summarized in Wagner and MacQueen's (1983) scheme: a flare induced disturbance illuminates low Alfvén speed regions in the legs of a CME in progress thus yielding a type II burst. The disturbance can later on overtake the CME. In contrast with this picture for coronal type II bursts, Cane et al. (1987) present evidence that radio emissive shocks in the interplanetary space are probably driven by energetic CMEs acting as pistons.

3 How to See a CME by Radio Methods?

The radio detection of CMEs is a largely unexplored territory (Bastian, this volume). It is an attractive challenge to detect CMEs by radio methods not only near the limb but also on the disk. There are only a few events studied commonly in radio and coronographic images due to the complexity of the problem and the lack of simultaneously working appropriate coronographs and radio telescopes. Available data mostly suffer from insufficient time and spectral coverage. Here we intend to summarize direct and indirect radio signatures of CMEs as follows:

- A direct hint for a CME means a radio phenomenon figures out (partly or completely) the body of a CME.
- An indirect hint for a CME is given if preexisting radio sources are influenced / activated / associated with additional effects in a typical manner.

3.1 Direct Methods

Two approaches are possible:

- Detection of the CME by observing the radio counterpart of the features visible in coronograph images in its thermal radio emission.
- Detection of nonthermal radio emission associated with parts of the CME.

CMEs in Thermal Radio Emission. The detection of a CME as near as possible to its origin by imaging its incoherent radio emission (thermal free-free or gyroresonance emission) seems to be a difficult task due to the fact that the contrast between the CME and the background corona is not very strong at least during the beginning of its rise. The best choice might be difference images revealing the CME due to the movement of some structural features. Only two case studies have been reported in the literature (Sheridan et al. 1978, Gopalswamy and Kundu 1992, 1993). Sheridan et al. (1978) have seen a bulge in the quiet sun map at 80 MHz at the site of a simultaneously appearing white light transient and estimated a fourfold density

excess from the radio data. Gopalswamy and Kundu (1992) found a laterally archlike extended enhancement at frequencies between 80 and 50 MHz resembling the optical CME feature which earlier passes the plasma levels observed by the imaging instrument. In this case, the radio source was not moving. Gopalswamy et al. (1996) traced the thermal microwave emission of a slowly erupting prominence which trails a "frontal loop - cavity" - CME pattern seen in YOHKOH SXT images.

Gopalswamy and Kundu (1992) give a CME mass estimate basing on the thermal bremsstrahlung process. Of course this method suffers from the same geometrical (unknown) parameters as mass estimates from white light images. The main problem is the superposition of CME- or flare related nonthermal radio sources which are stronger and hide the fainter thermal emission for the sensitive imaging instruments. On the other hand just these stronger nonthermal components are mostly the only sign of a CME in full disk patrol radio observations. In the following some attention is paid to these effects.

CMEs Traced by Nonthermal Radio Emission. A direct method to see CMEs in radio is tracing a nonthermally radio emitting component which can be associated with a CME (e.g. Hildner et al. 1986). Nonthermal radio emission evidences the presence of nonthermal electrons moving in or along a preexisting coronal (magnetic field) structure. Of course, nonthermal radio emission is also observed during solar flares. With regard to our initial remark (Section 2.1 and Figure 1a) about the different spatial scales of flares and average CMEs one must be careful with directly claiming evidence for having seen a CME without an independent confirmation.

A typical example is tracing plasma or gyrosynchrotron emission of the archlike or plasmoidlike moving type IV burst source (e.g. Stewart et al. 1982, Gopalswamy and Kundu 1989, Klein and Mouradian 1991). The moving type IV burst can sometimes be associated with the densest features visible in white light transients. However as with type II bursts the relationship between moving type IV sources and CMEs is still very unclear (Pick and Trottet 1988, Klein 1995). Aurass and Kliem (1992) draw the attention to a certain kind of type IV bursts with a characteristic late decimetric continuum pulse including a lot of spectral fine structures. They relate this observation to the disruption of the current flowing through the disconnected rising filament.

There are some reports about nonthermal phenomena which can be understood as the radio illumination of a CME by flare accelerated electrons. An example was given by Aurass et al. (1986), see Figure 8. With a time delay of 40 min, at two observing frequencies - 113 and 64 MHz - appears a morphologically highly similar pattern on the flux records. The corresponding

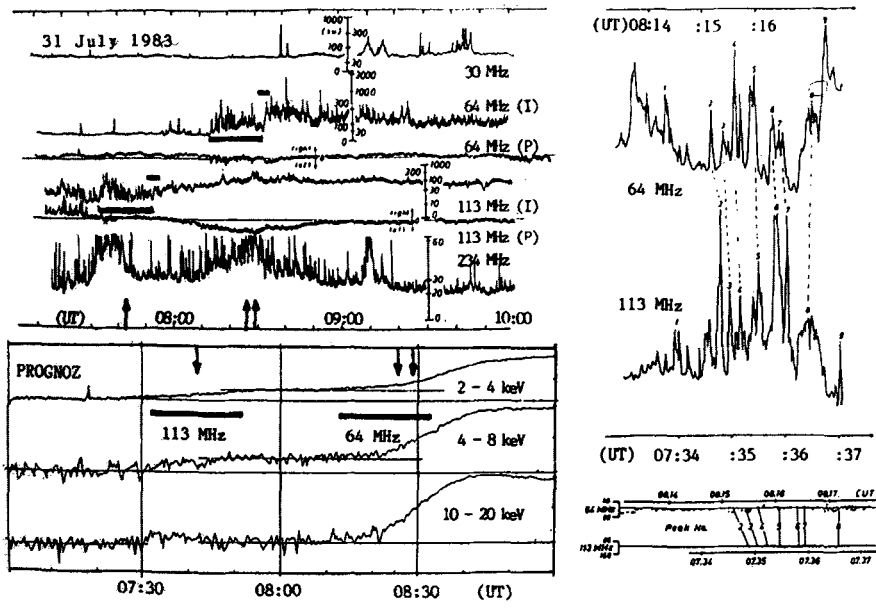

Fig. 8. Repetitive nonthermal radio bursts revealing the movement and the expansion of a long-living coronal structure on July 31, 1983 (Aurass et al. 1986).
Top left: the flux records, bars mark reappering intervals at 113 resp. 64 MHz. Arrows give times of subflares in the related active region. Right: High time resolution records of associated parts of both intervals, note the 40 min time delay and the time scale expansion. Bottom right: the spectral records of Weissenau confirm the narrow bandwidth of the effect. Bottom left: The soft X-ray records (PROGNOZ).

plasma levels have a radial distance of about 0.3 $R_\odot$. Comparing high time resolution records of these narrow band patterns at both frequencies reveals a time scale expansion between the observation at 113 and 64 MHz. A volume expansion rate of 0.2 - 1.2 % per minute has been estimated. The tail of the pattern expands faster than the head. The expansion is of the same order as for the giant X-ray arches analysed by Švestka et al. (1995), see Section 2.1. Because of the type I burst-like bandwidth of the patterns plasma emission is the relevant mechanism. The radio emission could be excited by nonthermal electrons enhancing plasma wave turbulence which is scattered directly into transversal waves at the clumpy, inhomogeneous medium represented by the CME (Melrose 1980). A confirmation of our interpretation was given by PROGNOZ soft X-ray data. During the appearance time of the flux patterns

at the two different plasma levels subflares were reported. They are associated with faint soft X-ray enhancements. This is in some way similar to the results of Lantos et al. (1981) who showed a clear temporal association between narrow band coronal plasma emission and an soft X-ray burst. In our case, between the first and the second "illumination" the coronal structure moves outward. A speed of 90 $\mathrm{km\,s^{-1}}$ was estimated well within the range of CME velocities. What is conservatively and cautiously called "strange reappearing noise storm chains" in Aurass et al. (1986) was probably a flare induced radio illumination of parts of a CME.

3.2 Indirect Methods

Here we investigate two possibilities:

- A characteristic change of a preexisting noise storm continuum possibly accompanied or followed by a gradual microwave burst.
- A repeated appearance of groups of type III and reverse drift bursts with spatially distributed but simultaneously acting sources.

Changes of Preexisting Noise Storm Sources. Noise storms (Elgarøy 1977) consist of long duration (hours to days) enhanced and smoothly varying meter wave (about 50 - 500 MHz) continuum emission. Superposed to the continuum component are the type I bursts, an ensemble of short time and narrow band emission pulses. Noise storms reveal a long duration nonthermal energy release outside flares (Klein 1995) above magnetically complex active regions. They have different starting frequencies and overall bandwidth if their onset is flare- or non-flare-associated (Böhme 1993). Due to the long duration of noise storms and their frequency range - which corresponds to the height range in which CMEs are initiated - a disturbance of a noise storm by an (independent) CME is not improbable. There are reports in the literature about diffuse brightness enhancements in white light associated with noise storms source regions (Kerdraon and Mercier 1982, Kerdraon et al. 1983). From case studies it is known that noise storms can be stimulated, but also suppressed by flares and by CMEs.

Aurass et al. (1993, and references about flare related effects therein) have shown that chromospheric matter evaporated during a flare was rising with about 300 $\mathrm{km\,s^{-1}}$ and has suppressed a preflare noise storm continuum. The resulting radio spectrum shows a type II burst in absorption. Chertok (1993) and Kahler et al. (1995) point the attention on a typical sequence of events in association with CMEs:

- A preexisting noise storm starts to grow. The growth has a duration of about 10 minutes and appears with a negative drift rate corresponding with an apparent speed of some tens of $\mathrm{km\,s^{-1}}$.

- The noise storm significantly decays within some minutes over a broad frequency range.
- In the same time interval a microwave burst starts to grow, sometimes with significant onset time delay from low to high frequencies. The microwave burst has no impulsive component, is not simply correlated with a soft X-ray burst and is sometimes referred to as "post eruptive energy release" (e.g. Chertok 1993) or belonging to "gradual events associated with CMEs" (e.g. Klein 1995 and references therein).

The smooth and long lasting meter wave continuum changes are difficult to recognize in routine spectral records. They are much easier to detect with a grid of single frequency receivers.

In the example Figure 9 (which we can not discuss in detail, here) the above mentioned phases are visible in the following intervals:

- The noise storm growth resp. the superposition of a slowly negatively drifting new radio source between 500 and 100 MHz starting at about 10:30 UT.
- The noise storm cessation starting some minutes past 11 UT and best visible between 300 and 200 MHz and from 11:20 till 11:30 UT.
- The gradual decimeter - microwave burst starting between 11:08 and 11:14 UT in the frequency range 500 MHz till 35 GHz (A. Magun, pers. comm.).

In the CME / radio literature the period February 1986 is of special interest due to the simultaneous action of the SMM coronograph and the Clark Lake Meter Wave Radioheliograph in an essential period of solar activity (reports on 13 - 17 February 1986 e.g. in Gopalswamy and Kundu 1992, 1993, Smith et al. 1993, Gopalswamy et al. 1994, Hundhausen 1994 in his Figures 31 and 32). We present in Figure 9 an example for a switch-off of a noise storm situated above the north-west limb (NRH 169 MHz) by a large scale disturbance. We argue that this disturbance is related with a CME. Burkepile and St.Cyr (1993) report on late hints for such a CME which was not directly observed due to SMMs schedule. Unfortunately, the analysis of several events of the February 1986 activity complex is scattered in literature - a comprehensive homogeneous analysis of all available data of this period seems promising.

Reverse Drift Bursts Can Indicate Coronal Destabilization. Klein and Aurass (1993) and Klein et al. (1996) describe the destabilization of the corona above a complex of four active regions. The loss of stability has been announced by preceding groups of meter wave fast drift bursts with a characteristic source distribution in space. Three 1.5 min duration groups of drift bursts were observed between 100 and 170 MHz during 3.5 hours before a filament eruption (Figure 10, left for the spectra). The burst groups consist

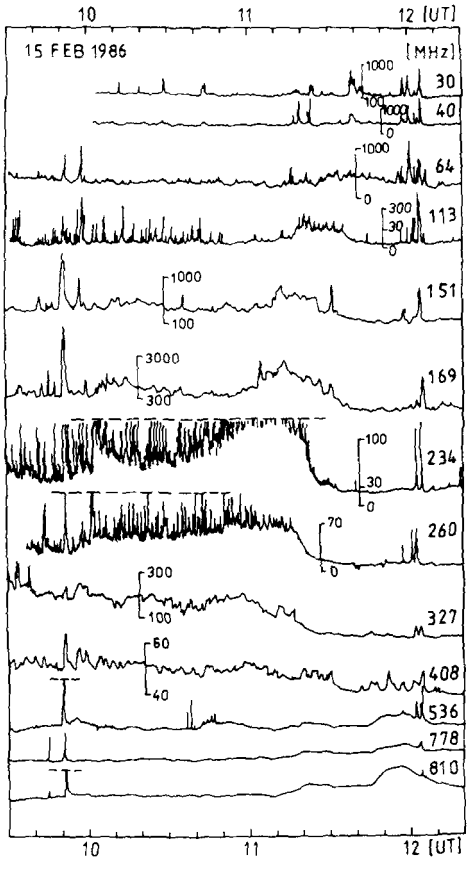

Fig. 9. The CME related noise storm enhancement, cessation and gradual microwave burst on February 15, 1986 around AR NOAA 4713 at the west limb. Single frequency records of Potsdam - Tremsdorf, NRH and AO Ondřejov, scales in solar flux units.

of type III bursts starting at frequencies larger than 165 MHz and of reverse drift (RS) bursts starting at about 120 MHz. We have drawn the RS burst sources as continuous crosses, the type III burst sources as stippled crosses over a composition of a Meudon H_α and a Mauna Loa coronograph image from the day before (from Klein et al. 1996). There are no white light CME observations available for the given day. As an inlay of Figure 10 right we show the involved active regions (among them two young regions displaying emerging flux).

Each of the spectrally simple RS bursts consists of two simultaneously brightening, widely displaced radio sources situated about 1 $R_\odot$ apart on both sides of a streamer-like configuration. This means the acceleration

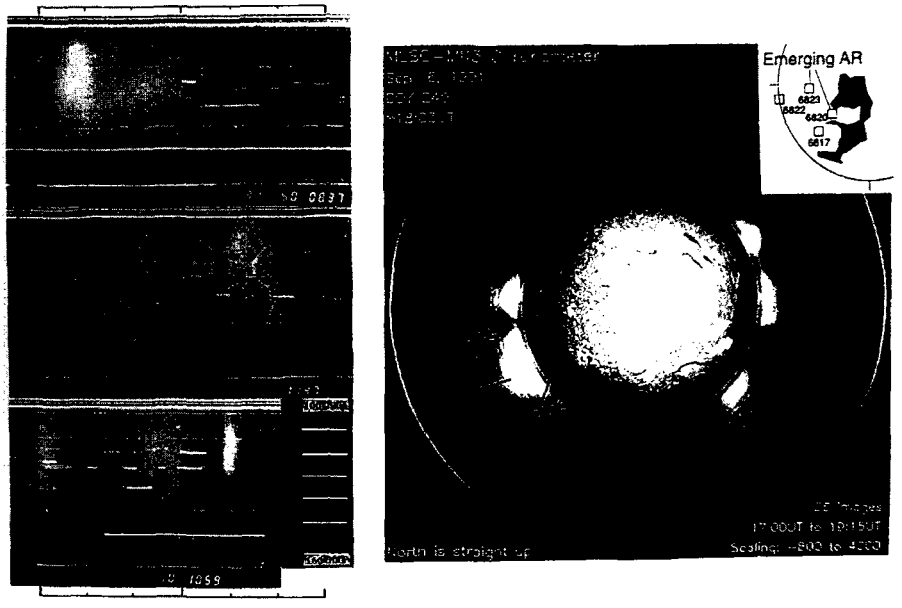

Fig. 10. Fast drift bursts in a destabilized part of the corona. Left : spectra 100 - 170 MHz, three time intervals from top to bottom, the bar denotes a two minute scale. Right: coronographic and H_α data; radio sources as crosses superposed. For details see text and Klein et al. (1996).

site of those electrons which become visible as RS drift burst is positioned at heights > 1 $R_\odot$ above the photosphere. In contrast, the type III burst sources are single ones and situated at the northern side of the streamer, only. The type III beam injection takes place at a nearly simultaneously acting acceleration site below 0.5 $R_\odot$. A filament eruption in NOAA AR 6817 past 12 UT, accompanied by a moving type IV burst, is the final signature of the destabilization of this part of the corona. During the observed process of reaction of the corona to continuous energy supply, small scale energy release processes were acting simultaneously in different heights of the involved part of the corona. Probably Klein et al. (1996) have seen what Sime (1989) described: "... CMEs represent rapid evolution of previously formed magnetic field structures through the gradual arrival of those structures at a state of instability which leads to rapid dynamical evolution."

4 Summary

We have tried to summarize the current knowledge about common aspects of white light CMEs and solar radio type II bursts. Several open questions have been assembled in this review:

- What is the large scale type II burst source pattern in relation with the CME body ?
- Can we confirm radio emission from quasi-transversal and quasi-parallel shock transitions ?
- Are coronal shocks driven by flare blast waves, by flare ejecta, or by a CME piston ?
- Are there relations between the spectral fine structure of type II bursts and the three aforementioned aspects ?
- Can we successfully revise the CME / type II speed / shock directivity problem ?
- What is the relationship between the time scales of nonthermal (radio) and thermal (soft X-ray) energy release during flare associated CMEs ?
- Are noise storm cessation events associated with gradual microwave bursts, and reverse drift bursts useful CME predictors ?
- Are further nonthermal radio phenomena (beneath the moving type IV bursts) associated with the process of magnetic disconnection of filaments, plasmoids and CMEs ? What happens during the onset and the decay of the moving type IV burst ?

The combined analysis of decimeter and meter wave radio observations from ground with the SOHO LASCO coronograph and YOHKOH SXT images can solve some of these problems.

Acknowledgements: The paper was improved by the patient and constructive criticism of an unknown referee and of the editor, Dr. G. Trottet. The author gratefully acknowledges discussions with the late Dr. H.- W. Urbarz, as well as with Dr.s J. Burkepile, H.-T. Claßen, E. Cliver, A. Klassen, K.- L. Klein, G. Mann, N. Vilmer and E.Ya. Zlotnik. Further, he is grateful to M. Karlický, A. Magun and P. Zlobec for data supply. He thanks H. Detlefs, D. Scholz and B. Schewe for software support and help in preparing the figures, and the staff of Potsdam-Tremsdorf and Nançay Observatories for running the observations. The work was supported by the YOHKOH community with the generous access to the SXT data. The cooperation between the Paris-Meudon Observatory and the AIP was possible due to the travel grants 312/pro-bmft-gg (DAAD) and 94053 (MAE) within the German-French PROCOPE program. The visit of the author at the CESRA 1996 was supported by the Deutsche Forschungsgemeinschaft grant No. DFG/Au 106/6-1. Thanks are due to the organizers of this conference.

References

Aurass H. (1992): Annales Geophysica **10**, 359

Aurass H., Hofmann A., Kurths J., Mann G. (1986): Solar Phys. **107**, 129

Aurass H., Hofmann A., Magun A., Soru-Escaut I., Zlobec P. (1993): Solar Phys. **145**, 151

Aurass H., Klein K.-L., Mann G. (1994a): ESA-SP **373**, 95

Aurass H., Magun A., Mann G. (1994b): Space Sci. Rev. **68**, 211

Aurass H., Kliem B. (1992): Solar Phys. **141**, 371

Aurass H., Rendtel J. (1989): Solar Phys. **122**, 381

Averianikhina Y.A., Paupere M., Eliass M., Ozolins G. (1990): Astron.Nachr. **311**, 6, 367

Benz A.O., Thejappa G. (1988): A&A **202**, 267

Böhme A. (1993): Solar Phys. **143**, 151

Brückner G.E., Howard R.A., Koomen M.J., and 12 coauthors (1995): Solar Phys. **162**, 357

Bougeret J.L. (1985): in Tsurutani B.T. and Stone R.G. (eds.) "Collisionless Shocks in the Heliosphere", Rev. of Current Research, AGU GN-34, Washington D.C., 13

Burkepile J.T., St. Cyr O.C. (1993): NCAR/TN 369+STR, HAO, Boulder, Colorado

Cane H.V., Sheeley N.R., Jr., Howard R.A. (1987): JGR **92**, A9, 9869

Chertok I.M. (1993): Astron. Rep. **90**, 135

Pearson D.H., Nelson R., Kojian G., Seal J. (1989), ApJ **336**, 1050

Dryer M. (1994): Space Sci. Rev. **67**, 363

Dulk G.A. (1982): in Proc. CESRA Conf., Trieste, Italy, p. 356

Elgarøy Ø. (1977): Solar Noise Storms, Pergamon Press, Oxford

Gary D.E., Dulk G.A., House L.L., Illing R.M.E., Wagner W.J., McLean D.J. (1985): A&A **152**, 42

Gergely T.E., Kundu M.R., Erskine F.T., III, and 11 coauthors (1984): Solar Phys. **90**, 161.

Gopalswamy N., Hanaoka Y., Kundu M.R., Enome S., Lemen J.R., Akioka M., Lara A. (1996): APJ, submitted

Gopalswamy N., Kundu M.R. (1989): Solar Phys. **122**, 145

Gopalswamy N., Kundu M.R. (1992a): in Zank, G.P. and Gaisser, T.K. (eds.) Part. Acc. in Cosm. Plasmas, AIP Conf. Proc. **264**, 257

Gopalswamy N., Kundu M.R. (1992): APJ **390**, L37

Gopalswamy N., Kundu M.R. (1993): Solar Phys. **143**, 327

Gopalswamy N., Kundu M.R., St. Cyr O.C. (1994): APJ **424**, L135

Harrison R.A. (1991): Phil.Trans.Roy.Soc. London A**336**, 401

Harrison R.A., Hildner E., Hundhausen A.J., Sime D. (1990): JGR **95**, 917

Hiei E., Hundhausen A., Sime D. (1993): Geophys. Res. Letters **20**, 2785

Hildner E., Bassi J., Bougeret J.L., and 18 coauthors (1986): in Kundu M.R., Woodgate B.E. (eds.) Energetic Phenomena on the Sun, NASA CP-2439

Holman G.D., Pesses M.E. (1983): ApJ **267**, 837

Hudson H. (1995): http://isasxa.solar.isas.ac.ip/hudson/scratch/iau153paper.ps

Hundhausen A.J. (1993): Journ.Geophys.Res. **98**, A8, 13.177

Hundhausen A.J., Burkepile J.T., St. Cyr, O.C. (1994): JGR **99**, A4, 6543

Hundhausen A.J. (1995): Proc. High Energy Physics Conference, in press
Hundhausen A.J. (1994): in "The Many Faces of the Sun", to appear
Kahler S.W. (1991): ApJ **378**, 398
Kahler S.W. (1992): Ann.Rev.Astron.Astrophys. **30**, 113
Kahler S.W., Cliver E.W., Chertok I.M. (1994): in V. Rušin, P. Heinzl and J.-C. Vial (eds.), Solar Coronal Structures, VEDA Publ. Comp. Bratislava, p. 271
Kahler S.W., Sheeley N.R. Jr., Liggett M. (1989): ApJ **344**, 1026
Kahler S.W., Sheeley N.R. Jr., Howard R.A., Koomen M.J., Michels D.J. (1984): Solar Phys. **93**, 133
Kai K., Nakajima H., Kosugi T. (1983): PASJ **35**, 285
Karlický M., Odstrčil D. (1994): Solar Phys. **155**, 171
Klassen A. (1996): Solar Phys. **167**, 449
Klein K.-L. (1995): in Benz A.O., Krüger A. (eds.): Coronal Magnetic Energy Energy Release, Springer, Berlin, p. 55
Klein K.-L., Aurass H. (1993): Adv.Sp.Res. **13**, 9, 295
Klein K.-L., Trottet G., Benz A.O., Kane S.R. (1988): ESA SP-**285**, 157
Klein K.-L., Trottet G., Aurass H., Magun A., Michou Y. (1995): Adv.Space Res. **17**, 425, 247
Klein, K.-L. Aurass, H., Soru-Escaut I., Kalman B. (1996): A&A accepted
Klein K.- L., Mouradian Z. (1991): in Schmieder B. and Priest E. (eds.), Flares 22 Workshop on Dynamics of Solar Flares, Chantilly, France, p. 185
Kerdraon A., Mercier C. (1982): in Proc. CESRA Conf. Trieste, Benz A.O., Zlobec P. (eds.), 27
Kerdraon A., Pick M., Trottet G., Sawyer C., Illing R., Wagner W., House L. (1983): APJ **265**, L19
Kopp R.A., Pneuman G.W. (1976): Solar Phys. **50**, 85
Krall N.A., Trivelpiece A.W. (1973): Principles of Plasma Physics, McGraw-Hill, New York
Kundu M.R., Erickson W.C., Gergely T.E., Mahoney M.J., Turner P.J. (1983): Solar Phys. **83**, 385.
Kundu M.R., Gopalswamy N. (1992): in Švestka, Z., Jackson, B.V., Machado, M.E. (eds.), Eruptive Solar Flares, Springer, p. 268
Labrum N.R. (1985): in Dulk G.A., McLean (eds.), Solar Radio Physics, Cambridge Univ. Press, Cambridge, p. 155
Lantos P., Kerdraon A., Rapley G.G., Bentley R.D. (1981): A&A **101**, 33
Low B.C. (1993): Adv. Space Res. **13**(9), 63
Mann G. (1995a): in Benz A.O., and Krüger A. (eds.), Coronal Magnetic Energy Energy Release, Springer, Berlin, p. 183
Mann G. (1995b): J. Plasma Phys. **53**, I, 109
Mann G., Aurass H., Paschke J., Voigt W. (1992): ESA-Journal **P-348**, 129
Mann G., Claßen H.T., Aurass H. (1995): A&A **295**, 775
Mann G., Claßen H.T. (1995): A&A **304**, 576
Mann G., Klassen A., Claßen H.T., Aurass H., Scholz D., MacDowall R.J., Stone R.G. (1996): AIP preprint **95-26**, A&AS in press
Mann G., Klose S. (1995): in AGU 1995 Fall Meeting, Suppl. Eos **7**, F455
Mann G., Lühr H., Baumjohann W. (1994): JGR **99**, A13, 13315
McAllister A.H., Dryer M., McIntosh P., Singer H., and Weiss L. (1994): in Proc. of the Third SOHO Workshop, ESA **SP-373**, 315

McAllister A.H., Dryer M., McIntosh P., Singer H., and Weiss L. (1996): JGR **101**, A6, 13497
Melrose D.B. (1980): Space Sci. Rev. **26**, 3
Mouradian Z., Soru - Escaut I., Pojoga S. (1996): Solar Phys. **158**, 269
Nelson G.J., Melrose D.B. (1985): in Dulk G.A., McLean D.J. (eds.), Solar Radio Physics, Cambridge Univ. Press, Cambridge, p. 333
Pick M., Trottet G. (1988): Adv. Space Res. **8**, 11, 21
Robinson R.D. (1985): Solar Phys. **95**, 343
Sheeley N.R., Stewart R.T., Robinson R.D., Howard R.A., Koomen M.J., Michels D.J. (1984): ApJ **279**, 839
Sheridan K.V., Jackson B.V., McLean D,J., Dulk G.A. (1978): PASA **3**, 249
Sime D.G. (1989): JGR **94**, A1, 151
Smith K..L., Švestka Ž., Strong K., McCabe M.K. (1993): Solar Phys. **149**, 363
Steinolfson R. (1992): Proc. 26th ESLAB Symp., ESA SP-**346**, 51
Stewart R.T., Dulk G.A., Sheridan K.V., House L.L., Wagner W.J., Sawyer C., Illing R. (1982): A&A **116**, 217
Švestka Ž. (1976): Solar Flares, Reidel, Dordrecht.
Švestka Ž., Farnik F., Hudson H., Uchida Y., Hick P., Lemen J.R. (1995): Solar Phys. **161**, 331
The Radioheliograph Group (1993): Adv.Space Res. **13**, 9, 411
Tsuneta T. (1996): ApJ **456**, 840
Tsuneta S., Acton L., Bruner M., and 10 coauthors (1991): Solar Phys. **136**, 37
Uchida T. (1974): Solar Phys. **39**, 431
Vršnak B., Ruždjak V., Zlobec P., Aurass H. (1995): Solar Phys. **158**, 331
Vilmer N., Trottet G., Barat C., and 5 coauthors (1993): in Advances in Solar Physics, ed. by G. Belvedere, M. Rodonò, G. Simnett, Lecture Notes in Physics **432**, 197.
Wagner W.J., MacQueen R.M. (1983): A&A **120**, 136
Webb D.F. (1994): in J. Bergeron (ed.), Reports on Astronomy, **XXIIA**, p. 64
Webb D.F., Forbes T.G., Aurass H., Chen J., Martens P.C.H., Rompolt B., Rušin V., Martin S.F. (1994): Solar Phys. **153**, 73
Webb A.H., Howard R.A. (1994): JGR **99**, A9, 4201
Weiss A.A. (1963): Australian J. Phys. **16**, 240